

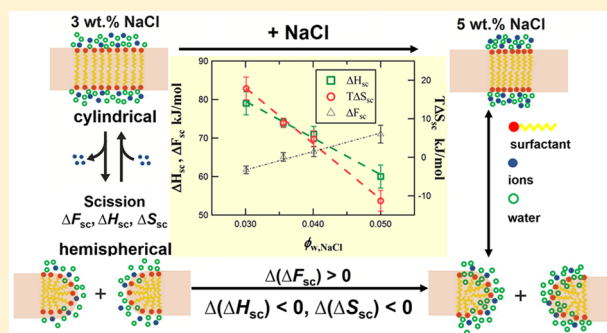
Enthalpy and Entropy of Scission in Wormlike Micelles

 Hanqiu Jiang,[†] Karsten Voggt,[†] Jacqueline B. Thomas,[‡] Gregory Beaucage,^{*,†} and Andrew Mulderig[†]
[†]Department of Chemical and Materials Engineering, University of Cincinnati, Cincinnati, Ohio 45221-0012, United States

[‡]P&G Analytical Sciences, 8700 Mason-Montgomery Road, Mason, Ohio 45040, United States

Supporting Information

ABSTRACT: The free scission energy is the thermodynamic parameter that governs the contour length of wormlike micelles (WLMs). It is the contour length and the propensity to coil and entangle that determine the viscoelastic properties of this commercially important substance class. The free scission energy ΔF_{sc} and the associated change in enthalpy ΔH_{sc} and entropy ΔS_{sc} on scission have been determined for a mixed anionic/zwitterionic surfactant system (sodium laureth sulfate and cocamidopropyl betaine) at various salt concentrations (3–5 wt % NaCl). Both enthalpy ΔH_{sc} and entropy ΔS_{sc} changes decrease linearly with increasing NaCl concentration. At NaCl concentrations above 4 wt %, ΔS_{sc} even adopts negative values. The term $T\Delta S_{sc}$ decreases more rapidly than ΔH_{sc} around room temperature and causes the observed elongation of WLMs upon addition of NaCl. It is suggested that ΔS_{sc} is initially positive due to fewer bound counterions per surfactant molecule at end caps compared to the intact, cylindrical parts before scission, leading to a net release of ions upon scission. Negative values of ΔS_{sc} are attributed to hydrophobic hydration occurring at the end caps at high salt concentrations. ²³Na NMR measurements indicate the presence of immobilized ions, supporting a previously proposed ion-cloud model based on neutron scattering results.



INTRODUCTION

Surfactant molecules with hydrophilic head-groups and hydrophobic tails may self-assemble into aggregates, known as micelles, in aqueous solution.¹ Micelles do not have a fixed structure, they constantly form and disrupt structure in a dynamic equilibrium.^{2,3} The equilibrium is controlled by a balance between the repulsive interactions of head-groups and the attraction of hydrophobic tails.⁴ These properties are related to the chemical nature of surfactant molecules and are often altered through the addition of salt or other additives.⁵ Inorganic salt is a particularly important additive used industrially to screen the electrostatic repulsions between surfactant head-groups and enhance the formation of elongated micelles.⁶

In the past decades, the impact of inorganic salts on micellar formation has been extensively studied and reported.^{7–11} Various techniques, such as rheology and scattering, were employed in these studies. It is well known that the addition of halide salts may induce a depression of the critical micellar concentration and the transition of micelle geometry from spheres to rods of increasing length to flexible wormlike structures. These changes may be induced by the reduction of electrostatic repulsion as well as hydration between head-groups upon addition of counterions.

The growth of WLMs relies on an increase in the end cap energy relative to the energy of a similar cylindrical section of WLM. This difference is proportional to the WLM scission

energy E_{sc} . The scission energy was defined in the mean-field theory of Cates and Candau by the following relationship¹²

$$\bar{N} = \phi^{1/2} \exp\left(\frac{E_{sc}}{2k_b T}\right) \quad (1)$$

where \bar{N} is the average number of surfactant molecules in a WLM, ϕ is the surfactant's volume fraction, k_b is the Boltzmann constant, and T is the absolute temperature in K. The equation is valid for neutral systems and has been successfully employed for those that are highly electrostatically screened.¹³ However, there are few reported values in the literature for E_{sc} .^{13–25} Most of the reports^{14,16–25} employ rheology to determine the scission energy indirectly using a relation between the activation energy of breakage and the terminal relaxation time. Values between 50 and 120 kJ/mol are found for E_{sc} depending on the amphiphile type and solvent condition. However, Couillet et al. point out that high values of E_{sc} lead to unrealistically large values for the contour length.²³ They suggest that E_{sc} is more accurately a free energy consisting of an enthalpic and an entropic part, and that the Arrhenius plots employed in the rheology-based method miss the entropic contribution. In a recent work, we scrutinized [relation 1](#) and the possibility for an entropic contribution to

Received: August 28, 2018

Revised: October 18, 2018

Published: October 23, 2018

E_{sc} .^{13,13} It was found that the introduction of a term $T\Delta S_{sc}$ indeed yields more realistic and consistent contour lengths. The Gibbs free energy of scission can be formulated as

$$\begin{aligned} \Delta F_{sc} &= 2RT \ln \left(\frac{\pi R_1^2 L_1 z \rho_{WLM} N_A \times 10^{-24}}{m_{surf} \phi^{1/2}} \right) \\ &= \Delta H_{sc} - T\Delta S_{sc} \end{aligned} \quad (2)$$

where R is the gas constant, N_A is the Avogadro constant, T is the temperature in K, and ΔH_{sc} and ΔS_{sc} are the enthalpy and the entropy of the scission, respectively. The parameters m_{surf} , ρ_{WLM} , and ϕ_v are the mass of a single surfactant molecule in g/mol, the mass density of the micelles in g/cm³, and the volume fraction of the WLMs, respectively. The WLMs are envisioned as a chain of cylindrical subunits with a length L_1 and a radius R_1 in Å in this approach, summing up to a total number of subunits z . These structural parameters are determined by small-angle neutron scattering (SANS) using a hybrid scattering function, where the index “1” refers to the structure of the subunits, whereas the index “2” indicates parameters belonging to the global, overall chain structure²⁶ (see Section 2).

In the above-mentioned work, it was found that the enthalpy of scission for WLMs assembled from sodium laureth-1 sulfate (SLE1S) is higher at 3 wt % of NaCl than at 6 wt % of salt.¹³ This result is in qualitative agreement with findings from rheology-based studies on other surfactant systems.²³ The change in ΔS_{sc} with salt concentration, however, yielded an unexpected result. The entropy change on scission decreased with increasing salt concentration, exhibiting a negative value at 6 wt % of NaCl. This study seeks to put these results on a broader basis and scrutinize the different contributions by determining ΔF_{sc} for a mixed surfactant system at various temperatures and for a series of salt concentrations (3, 3.5, 4, and 5% of NaCl). The enthalpy change ΔH_{sc} and the entropy change ΔS_{sc} are determined according to eq 2 and possible molecular origins are discussed.

The mixed surfactant system consists of an anionic surfactant, SLE1S, and a zwitterionic surfactant, cocamidopropyl betaine (CAPB), which is commercially more relevant^{27–29} than pure SLE1S used in the previous study.¹³ Zwitterionic surfactants, such as CAPB, have been shown to lower the critical micellar concentration and enhance the micellar growth in anionic surfactant systems because of the strong synergistic effect of the surfactant mixture.^{29,30}

THEORY

The free scission energy ΔF_{sc} was considered temperature-independent in the original work of Cates, Fielding, and Candau,^{12,31} that is, it was designated as an enthalpy lacking any entropic contributions. However, this approach led to inconsistent results and unrealistically large contour lengths at high scission energies.^{13,23} The introduction of an entropic term ΔS_{sc} fixed this problem and led to consistent results under various salt and surfactant concentrations.¹³

However, the molecular/structural origin of the contributions of ΔH_{sc} and ΔS_{sc} remain obscure. ΔH_{sc} is found to decrease with increasing salt, which is somewhat counter-intuitive. Under high ionic concentrations, which are the usual case for WLMs, repulsive interactions between the surfactant head-groups are screened, so that one would expect ΔH_{sc} to be independent of salt concentration. In this case, ΔH_{sc} would be

dominated by the cylindrical cross-sectional area and the chemical nature of the WLM's hydrophobic core and hardly affected by changes in electrostatic head-group interactions. It was presumed in ref 13 that with increasing salt concentration, the mechanism of micelle breakage changes from predominantly chain scission at low salt concentration toward predominantly branch stripping at high salt concentrations because WLM branching is induced by increasing ionic concentration.¹³ This would shift the reaction process from a mechanism yielding two end caps, Figure 1, to one yielding

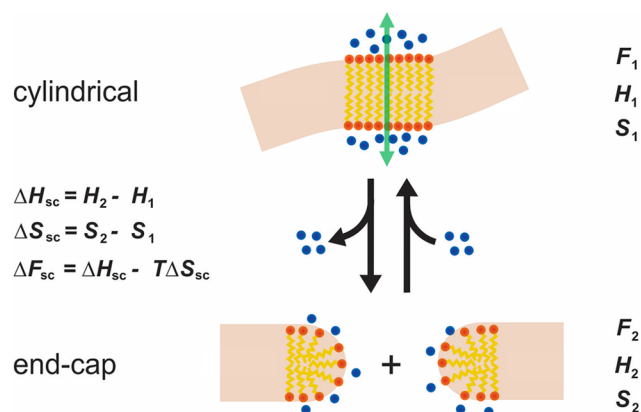


Figure 1. Scission via breakage of a cylindrical WLM segment. The cylindrical segment exhibits a larger surface charge density, so that the formation of two end caps induces the release of bound ions.

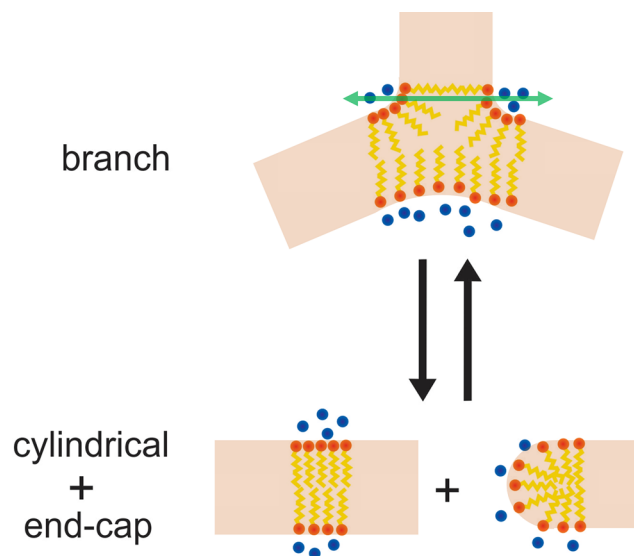


Figure 2. Micelle breakage via branch stripping from a branch point within a WLM. The creation of a single end cap in this case would lead to a lower overall enthalpy ΔH_{sc} as compared to the breakage mechanism given in Figure 1.

just a single end cap per scission, Figure 2. Provided the main energy required for chain breakage lies in the creation of the end cap, one would expect that ΔH_{sc} drops to about half its value upon changing from a scission to a branch stripping mechanism. Rheological and structural data indicate a branch formation in the according salt concentration range,^{13,26} so that this explanation seems plausible. However, the branch-

stripping model is qualitative and based on two values of ΔH_{sc} at different salt concentration (3 and 6 wt % NaCl). To put this hypothesis on a more solid foundation, one needs to show that ΔH_{sc} decreases proportionally to the branch content, n_{br}/z , where n_{br} is the number of branches per chain and z is the average number of subunits in a chain.

A surprising result is the occurrence of a negative entropy of scission, ΔS_{sc} , at high salt concentrations.¹³ Given that WLMs in solution exhibit densities similar to the surfactants in solid state (~ 1.1 g/mL^{28,13}), one can, in first approximation, neglect the entropy change upon scission of the WLM's hydrophobic core and attribute ΔS_{sc} solely to the changes in the organization of the associated (counter) ions. Indications for the presence of an ion cloud surrounding the WLMs have been demonstrated^{32,33} for the present mixed surfactant system. The number of ions associated with the WLMs scales linearly with the bulk concentration of salt. This finding will be further verified in this work by ²³Na nuclear magnetic resonance (NMR) measurements. It is known that end caps have a lower capacity of binding counterions due to their lower surface charge density.³⁴ The free energy required for the creation of two end caps thus includes the release of ions (see Figure 1). In this case, the immobilized or partially immobilized ions in the cloud would need to uptake heat from the environment to leave the ion cloud and become mobile bulk ions. Alternatively, one may formulate that the release of partially immobilized, i.e., "cold" ions into the bulk effectively decreases the ion's temperature. This heat transfer $\Delta Q/T$ from the environment in the direction of the WLM system at constant temperature and pressure would account for a positive entropy change from the perspective of the WLM dispersion. A positive entropy change on scission has previously been related to counterions.^{35,36}

The positive entropy change on scission can be explained using an ion-cloud model;³³ however, the occurrence of a negative scission entropy at high salt concentrations requires further explanation. Given the differences in ΔH_{sc} and ΔS_{sc} at high and low salt concentrations and just considering scission via breakage or branch stripping, there are two manifest sources for a negative ΔS_{sc} . First, depending on the ion-binding properties of branch points, the onset of branching may give rise to an uptake of ions upon branch stripping. If the ion-binding capacity of a given branch point is lower than that of the resulting cylindrical segment plus end cap (see Figure 2), then branch stripping would lead to the binding of ions and accordingly to a negative contribution to ΔS_{sc} .

Moreover, the increase in salt concentration may stabilize and increase the density of the WLM's cylindrical part more than at its end caps. If the addition of salt energetically favors the presence of surfactants in the densely packed cylindrical WLM segment, then the average number of surfactant molecules in the end caps decreases. This in turn would lead to an increased exposure of the hydrophobic hydrocarbon chains to water at the end caps. At room temperature, hydration of hydrophobic groups leads to a decrease in entropy,^{37–39} possibly due to the organization of water around hydrophobic groups. Moreover, both increase in hydrophobic hydration as well as the transfer of less surfactant molecules from the cylindrical environment into a hemispherical environment in the end cap at high salt concentrations would be expected to decrease ΔH_{sc} . Although entropically unfavorable, the hydration of hydrophobic residues is usually enthalpically favorable around room temperature.^{37,40}

The change in ΔS_{sc} for the NaCl concentration series can be explored to decide which of these two explanations, branch stripping or hydrophobic hydration, is more plausible. In ref 13 just two values at a higher (6.13%) and a lower (3.01%) NaCl concentration at 0.25% SLE1S are available for ΔS_{sc} (-61 ± 2 J/(mol K) for high salt, 100 ± 20 J/(mol K) for low salt) and ΔH_{sc} (-49.6 ± 0.5 kJ/mol for high salt, 87 ± 5 kJ/mol for low salt). This does not allow for the verification of an association of the change ΔS_{sc} with the onset/progress of branching. As outlined below, the utilization of SANS allows the assessment of the branch density, n_{br}/z , of WLMs. The determination of n_{br}/z and ΔS_{sc} for a NaCl concentration series can help to determine which of the two explanations given above, branch stripping or hydrophobic hydration, is in agreement with the observations.

Employing eq 2, ΔF_{sc} , ΔH_{sc} , and ΔS_{sc} can be determined from the structural properties of the WLMs, namely, their contour length L_2 and radius R_1 . In this process, the WLMs are modeled as chains with cylindrical segments, where the index 1 refers to the cylindrical subunits and the index 2 refers to the global, convoluted, and branched structure. Small-angle neutron scattering can be utilized to determine the structure. On the basis of a hybrid unified Guinier/power-law approach, the scattered intensity of WLMs can be separated according to their structural hierarchy.^{41,42,26}

$$I(q) = I_1(q) + I_2(q) \quad (3)$$

where $I(q)$ is the overall scattering intensity and $I_1(q)$ is the scattering intensity contributed by the cylindrical subunits the overall scattering intensities

$$I_1(q) = \int_0^\infty N(R_1) G_1 P_{cyl}(q, R_1, L_1) dR_1 \quad (4)$$

where $P_{cyl}(q)$ is the form factor for a cylinder.

A distribution function $N(R_1)$ accounts for polydispersity of the cross-sectional radius of the cylindrical subunits, R_1 . L_1 is the length of the cylindrical subunits. The value $G_1 = I_1(0)$ is given by $N/V(\Delta\rho)^2 V_{cyl}^2$, where N/V is the number density of cylindrical subunits, $V_{cyl} = (\pi R_1^2 L_1)$ is the volume of the cylinders and $\Delta\rho$ is the difference between the scattering length density ρ_{cyl} of the cylindrical subunits and the solvent ρ_s . $I_2(q)$ is the scattering intensity of the higher structural level with interconnected subunits that is formulated as follows

$$I_2(q) = G_2 e^{-(R_g^2 q^2)/3} + B_2 e^{-(R_g^2 q^2)/3} (q_2^*)^{-d_{f,2}} \quad (5)$$

where $q_2^* = \frac{q}{\text{erf}\left(\frac{1.06qR_g}{\sqrt{6}}\right)}$ and $\text{erf}(x)$ is the error function.

The scattering function is fully described by Vogtt et al.²⁶ Of special importance is the weight average number of subunits z that can be calculated from the scattered intensity at zero angle G_i for the structural levels $i = \{1, 2\}$.

$$z = \frac{G_2}{G_1} + 1 \quad (6)$$

Using z , the parameter n_{br} can be calculated as follows.⁴³

$$n_{br} = \frac{z^{(5/2d_{f,2}-3/2c)+(1-1/c)}}{2} - 1 \quad (7)$$

where $d_{f,2}$ is the fractal dimension of the WLM. The parameter c is the connectivity dimension $c = d_{f,2}/d_{\min,2}$, where $d_{\min,2}$ is the minimum dimension of the fractal-like object. For linear

WLMs, assuming a self-avoiding walk of the cylindrical subunits, $d_{\min,2} = 5/3$. The connectivity dimension $c = 1$ for unbranched WLMs and $c > 1$ for branched systems given that the formation of other structures than cylinders can be ruled out. For $d_{f,2} = 1.67$, $c = 1$ and the chains are unbranched or linear. For $d_{f,2} > 1.67$, the chains are branched.

With these parameters, the change in the scission entropy $\frac{d\Delta S_{sc}}{d\phi_{NaCl}}$ as well as the change in the scission enthalpy $\frac{d\Delta H_{sc}}{d\phi_{NaCl}}$ with the salt mass fraction can be compared with the development of branching. Then, the applicability of the possible explanations for the observed ΔS_{sc} and ΔH_{sc} can be evaluated.

MATERIALS AND METHODS

Surfactant mixtures were made from a mix of a common anionic surfactant, sodium laureth-1 sulfate (SLE1S, commercially available as STEOLCS-170) at 0.179 wt % (5.70 mM), and a zwitterionic surfactant, cocamidopropyl betaine (CAPB, commercially available as Amphosol HCA-HP) at 0.021 wt % (0.648 mM), with a molar ratio of 9:1 in deuterated water, as shown in Figure 3. (Both surfactants are

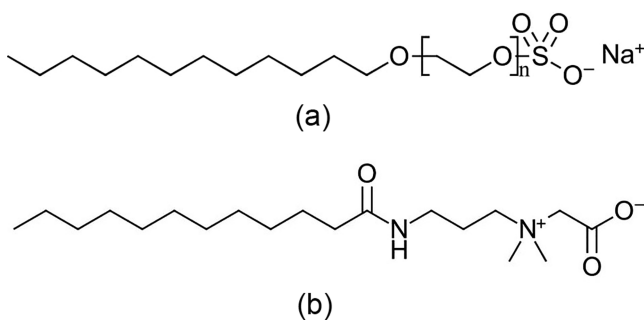


Figure 3. Surfactants used in this study. (a) Sodium laureth-1 sulfate (SLE1S) and (b) cocamidopropyl betaine (CAPB).

available from Stepan Chemical, Northfield, Ill.) This binary surfactant mixture was chosen because it has been seen to produce stable WLM structures and serves as a model for more complicated commercial surfactant mixtures. A series of salt concentrations, NaCl at 3.01, 3.56, 4.01, and 5.00 wt % (0.57, 0.67, 0.75, and 0.94 M), were investigated at three temperatures, 15, 25, and 35 °C. All measured samples are transparent and monophasic in the examined temperature range. The salt and surfactant concentration ranges were selected to ensure the presence of WLMs in dilute condition as shown in the pseudo-phase diagram given in Figure 4. At salt concentration around

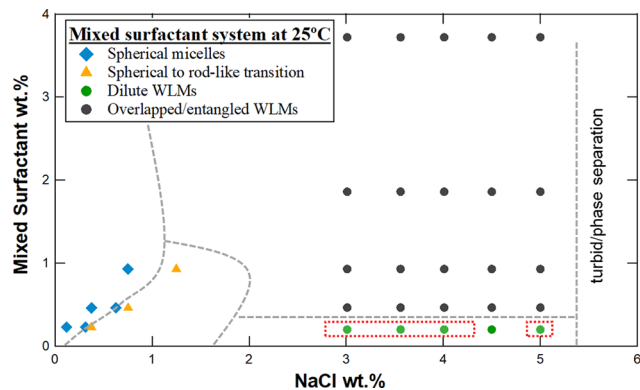


Figure 4. Pseudo-phase diagram of the studied mixed surfactant system at 25 °C. Gray dotted lines are drawn just for the guidance of eyes. Points highlighted with red dotted lines correspond to the samples in this study.

6%, the surfactant system becomes hazy and shows the tendency to phase separate. Data points in Figure 4 are evaluated based on the SANS results from the measured samples. The corresponding scattering profiles have been plotted selectively in Figure S4 of the Supporting Information.

SANS data were measured on the GP-SANS instrument at Oak Ridge National Laboratory, Oak Ridge, TN. Data were reduced by procedures provided by the beam line. Data sets after reduction and background correction were fitted as described in ref 26. Previous SANS data of a concentration series³³ have shown that samples at a weight fraction of 0.2% are sufficiently dilute to avoid any overlap between WLMs.

NMR measurements were performed to verify the premise of the ion-cloud model³³ that ions are immobilized near the micelles in numbers far greater than a monolayer, and that this ion cloud does not display saturation. NMR samples were prepared by placing Na⁺/surfactant solutions in 5 mm NMR tubes. An external reference standard of Na₇Dy(PPP)₂ ([Na⁺] = 0.40 M) in a coaxial 2 mm NMR tube was then inserted for each experiment. A $\Pi/2$ pulse length of 16 μ s was measured and used for all ²³Na NMR experiments. The experiments were performed at 25 °C and recorded at 105.84 MHz on a Bruker Avance III 400 MHz (9.4 T) spectrometer equipped with a 5 mm broadband probe. The same NMR parameters and data analysis were adopted for single-quantum (SQ) and double-quantum filtered (DQF) experiments as reported in previous studies.^{44–46} For each sample, SQ and DQF experiments were recorded with an identical number of scans (64), repetition times, and receiver gains. The SQ and DQF spectra were processed and analyzed using MestReNova software (Mestrelab Research, S.L., Santiago de Compostela, Spain).

RESULTS AND DISCUSSION

Figure 5 is a log–log plot of scattered intensity versus scattering vector for samples with increasing NaCl concentration.

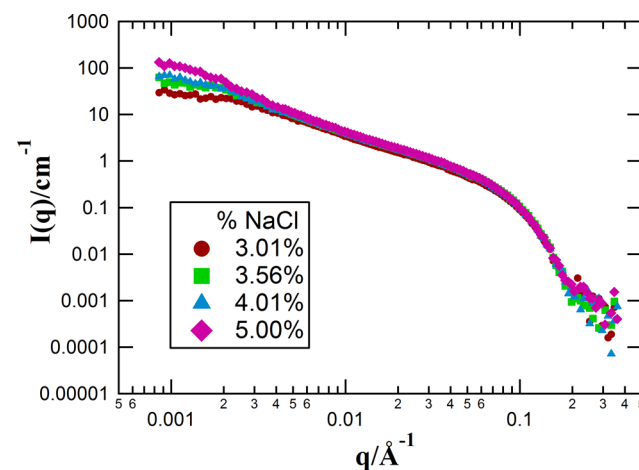


Figure 5. Log–log plot of scattered intensity versus scattering vector for samples with 0.2% MS at 25 °C with varying NaCl concentrations.

at 25 °C and a fixed surfactant concentration of 0.2%. (Figures S1–S3 in the Supporting Information give similar scattering curves measured at 15 and 35 °C as well as the fitting values.) Overlap of the scattering curves at high and intermediate q indicate that there are only slight differences in the cylindrical subunit structure with increasing salt concentration. The main difference is the contour length of WLMs and is visible in the pronounced changes in $I(q)$ at low- q .

The increase in scattered intensity at low- q is related to a monotonic increase in contour length in salt concentration. Samples with 0.2% mixed surfactant are dilute as determined

from a concentration series.³³ The large-scale structural features (L_2 and z) for the samples at higher salt concentration have relatively large error bars, as given in Table S1 in the Supporting Information, because the changes occur at the lower q -limit of the SANS instrument. The micellar contour length (L_2), as well as number of cylindrical subunits (z), was found to increase with salt concentration, whereas opposite trend was observed with increasing temperature. The length of cylindrical subunits, L_1 , is around 600 ± 100 Å. Variations in L_1 at different temperatures and salt concentrations are small. The radius of the micelles remains constant with respect to salt concentration and becomes slightly smaller at higher temperatures. From these parameters, the average number of surfactants in a micelle (\bar{N}) can be determined.¹³ \bar{N} , in turn, allows the calculation of ΔF_{sc} .

The free energies of scission are calculated based on eq 1 and plotted against temperature as shown in Figure 6. A linear

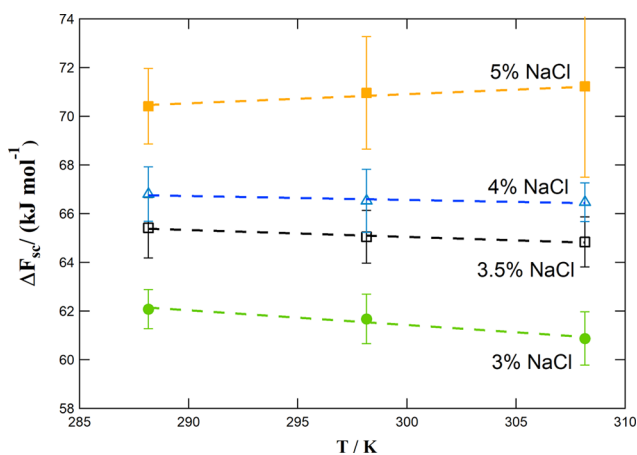


Figure 6. Free energy of scission ΔF_{sc} as a function of temperature at a constant surfactant weight fraction of 0.2% with 5% (■), 4.01% (Δ), 3.56% (□), and 3.01% (●) NaCl.

relationship between ΔF_{sc} and temperature is observed at all salt concentrations. Note that the error bars depict the maximum expected inaccuracy as calculated from the error propagation based on the SANS counts. The enthalpy and entropy of scission are obtained through fits of ΔF_{sc} based on eq 1. They are summarized in Tables 1 and 2. ΔF_{sc} has only

Table 1. Free Energy, Enthalpy, and Entropy of Scission of 0.2% Mixed Surfactant with Various Salt Concentrations at 15, 25, and 35 °C

NaCl (wt %)	T (°C)	ΔF_{sc} (kJ/mol)	ΔH_{sc} (kJ/mol)	ΔS_{sc} (J/(mol K))
3.01	15	62.1 ± 0.8	79 ± 3	60 ± 10
	25	61.7 ± 1.0		
	35	60.9 ± 1.1		
3.56	15	65.4 ± 1.2	74 ± 1	30 ± 4
	25	65.1 ± 1.1		
	35	64.8 ± 1.0		
4.01	15	66.8 ± 1.1	71 ± 2	16 ± 7
	25	66.5 ± 1.3		
	35	66.4 ± 0.8		
5.00	15	70.4 ± 1.5	60 ± 3	-38 ± 9
	25	71.0 ± 2.3		
	35	71.2 ± 3.7		

Table 2. n_{br} and n_{br}/z of 0.2% Mixed Surfactant with Various Salt Concentrations at 15, 25, and 35 °C

% NaCl	T (°C)	z	n_{br}	n_{br}/z
3.01	15	11 ± 2		
3.56	15	26 ± 6		
4.01	15	40 ± 8	0.3 ± 0.2	0.008 ± 0.002
5	15	80 ± 20	0.6 ± 0.2	0.0075 ± 0.0007
3.01	25	8 ± 1		
3.56	25	14 ± 2		
4.01	25	18 ± 3	0.1 ± 0.3	0.006 ± 0.03
5	25	50 ± 20	0.5 ± 0.4	0.010 ± 0.004
3.01	35	5 ± 1		
3.56	35	10 ± 1		
4.01	35	13 ± 1		
5	35	40 ± 10	0.5 ± 0.4	0.013 ± 0.004

slight variation with temperature. The absolute values at different salt concentrations differ significantly. A decrease in both ΔS_{sc} and ΔH_{sc} with salt concentration is observed. As $T\Delta S_{sc}$ decreases more rapidly compared to ΔH_{sc} , the overall ΔF_{sc} increases with increasing NaCl concentration as does the average contour length.

The average number of surfactant molecules per WLM, \bar{N} , is given as a function of salt concentration and temperature in Figure 7. As expected, $\bar{N} \propto L_2$ is smaller for higher

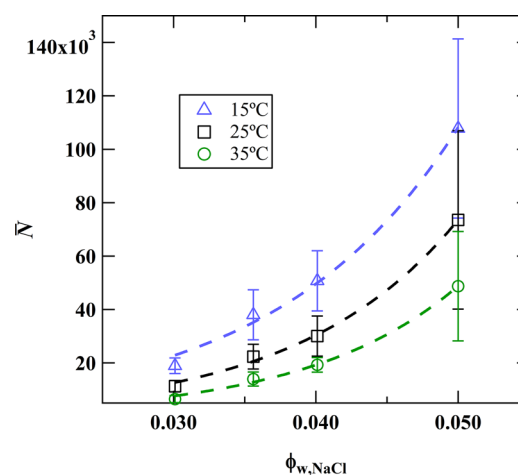


Figure 7. Average number of surfactants contained in a micelle versus NaCl weight fraction. The dashed lines follow eq 1 under the assumption that the scission energy is linear in salt concentration.

temperatures and increases exponentially with increasing salt concentration since ΔF_{sc} is linear in $\phi_{w,NaCl}$ and eq 1 predicts an exponential dependence of \bar{N} on ΔF_{sc} . At low surfactant concentration, the contour length L_2 is the main factor governing the viscoelastic behavior. With these values of \bar{N} , L_2 , and R_1 , a surfactant head-group area of 50 Å² is calculated, in very good agreement with literature values for the very similar surfactant sodium dodecyl sulfate.⁴⁹

Figure 8 depicts the influence of the weight fraction of salt $\phi_{w,NaCl}$ on the contribution of scission enthalpy ΔH_{sc} and entropy $T\Delta S_{sc}$ to the total free energy of scission ΔF_{sc} . Within the observed accuracy, the changes are linear. A positive enthalpy change on scission means that the surfactant molecules in the end caps have a higher internal energy than those on the cylindrical body, which is consistent with previous studies using rheological methods.^{13–25} This enthalpy change

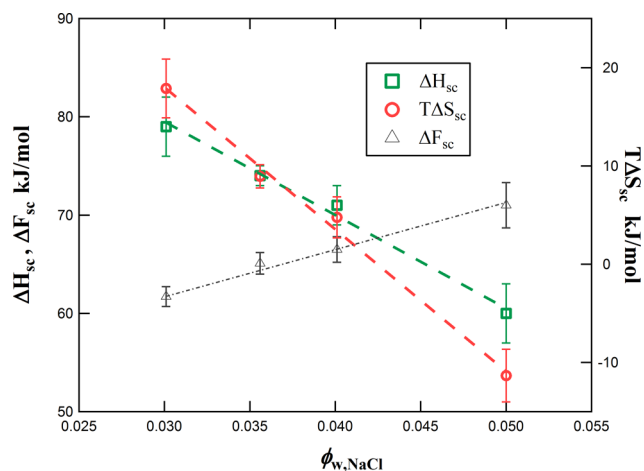


Figure 8. Enthalpic (ΔH_{sc}) and entropic ($T\Delta S_{sc}$) contributions to the overall free energy of scission (ΔF_{sc}) as a function of NaCl weight fraction at 25 °C. The more rapid decay of $T\Delta S_{sc}$ compared to ΔH_{sc} leads to an increase in ΔF_{sc} and growth in micellar length.

on scission decreases with increasing salt concentration, consistent with ΔH_{sc} previously reported for the pure SLE1S system.¹³ However, the overall moderate change in ΔH_{sc} between 3 and 5 wt % NaCl of about 25% is not compatible with the branch-stripping explanation given in the previous work.¹³ Although ΔH_{sc} decreases continuously in a linear manner, the branching sets in at 4 wt % NaCl as visible from n_{br} , average number of branch points per micelle, and n_{br}/z , number of branches per Kuhn unit, as shown in Table 2. Below this NaCl concentration, there is no reason to assume the presence of branches despite the large error bars for n_{br} . The fact that ΔH_{sc} decreases in the absence of branches rules out branch stripping as a competitive scission mechanism that causes the decrease in enthalpy of scission.

In a similar manner, the impact of branch points on the change in ΔS_{sc} can be ruled out. ΔS_{sc} decreases likewise continuously even in the absence of branches, reaching $\Delta S_{sc} \approx 0$ at about 4.2 wt % NaCl and becomes negative at a higher salt concentration. Accordingly, the more likely explanation is the

increase in hydrophobic hydration at the end caps rather than the onset of branch stripping.

The hydrophobic hydration model has the advantage that it can explain both $\frac{d\Delta S_{sc}}{d\phi_{NaCl}}$ and the change in the scission enthalpy

$\frac{d\Delta H_{sc}}{d\phi_{NaCl}}$ without making additional assumptions on putative properties of branch points. The expected stabilization of the cylindrical WLM sections with more bound ions at higher salt level relative to end caps suffices as an explanation for both (see Figure 9). As indicated by both ion-cloud model and ²³Na NMR results, which will be discussed below, addition of NaCl leads to the binding of more ions per surfactant molecule and a denser, energetically more stable packing of the cylindrical geometry. Stabilization of the cylindrical sections decreases the number of surfactants per end cap. Scission at high salt concentration leads accordingly to end caps with fewer surfactant molecules. The loosely packed end caps are more exposed to water, leading to more pronounced hydrophobic hydration, i.e., increasingly negative entropy ΔS_{sc} . Alternatively, one may envision the hemispherical end caps at high salt concentration as swollen by radial displacement of surfactant molecules and penetration of water molecules, which would exhibit the same result. It can be said that hydrophobic hydration increases with increasing NaCl concentration at the end caps because this effect alone has been observed to lead to the trends of ΔH_{sc} and ΔS_{sc} with salt concentration.

The model outlined above necessarily requires the presence of two ion populations, bound and free, to explain the observed entropy changes. It has been shown that ²³Na NMR spectroscopy is a useful technique in characterizing sodium mobility in various systems.^{44,45,47,48} Theoretically, the total sodium population (both restricted and unrestricted) is measured using SQ experiments, and DQF experiments filter out the signal from the unrestricted sodium ions and therefore are a direct measure of the “bound” sodium ions.

Measurements to assess the mobility of the sodium ion population have been performed. ²³Na SQ and DQF spectra of mixed surfactant samples with increasing salt concentration are plotted in Figure 10. The peak with negative dips in the DQF

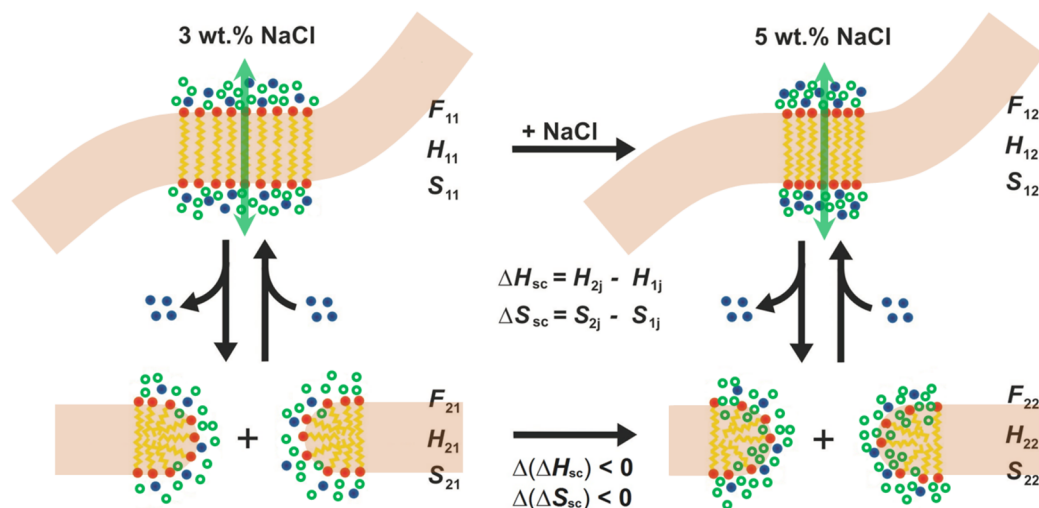


Figure 9. Sketch of the hydrophobic hydration model with increasing salt concentration. The sketch shows bound counterions (blue circles) and water molecules (green circles). $\Delta(\Delta H_{sc})$ and $\Delta(\Delta S_{sc})$ denote the difference of scission enthalpy and entropy change between 3 and 5 wt % NaCl, respectively.

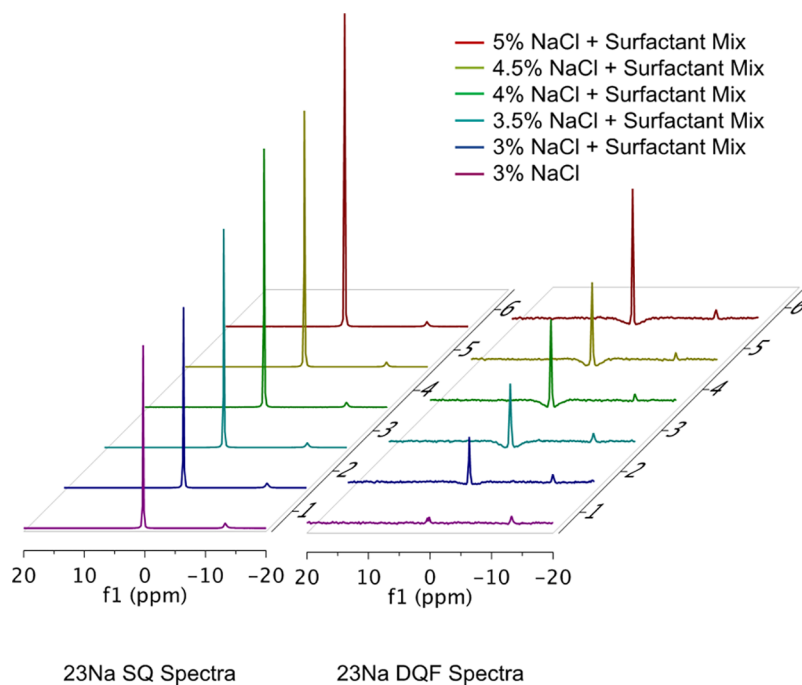


Figure 10. Stacked plot of ^{23}Na SQ (left) and DQF (right) NMR spectra of 0.2% mixed surfactants system in D_2O with varying NaCl concentration. The smaller second peak present in all the spectra were contributed by the external standard. Only one control sample is shown for clarity.

spectra is a typical feature indicating the presence of bound ions.^{44–46}

The molar concentration of Na^+ was determined from the area under the peak of SQ spectra and normalized by the signal of the external reference. The obtained Na^+ molar concentrations were converted to NaCl weight fractions (3.1, 3.6, 4.6, 4.8, and 5.4%) show good agreement with the sample fabrication values (3.01, 3.56, 4.01, 4.5, and 5%). As expected, the samples in the presence and absence of surfactant at the same salt level have very similar ^{23}Na SQ spectra, shown on the left of Figure 10, indicating that the presence of surfactant does not affect the acquisition of the Na^+ resonance signal. The bound fraction of Na^+ was determined by the ratio of the integration of the DQF signal to that of the SQ signal. Theoretically, if only free Na^+ is present in the measured solution (pure salt solution), a flat line without a peak is expected for the DQF spectrum. However, due to high Na^+ concentration, a small contribution was observed in the control samples (bottom right spectrum in Figure 10, average $12 \pm 2\%$), which was accounted for in the reported values.

Figure 11 shows the dependence of the bound fraction (DFQ) of Na^+ (red circles and left axis) as a function of the overall weight percent Na^+ (SQ). The bound fraction (DFQ) of Na^+ is the number of bound Na^+ divided by the number of all Na^+ in the system. Based on the ion-cloud theory,³³ this value should remain constant with increasing salt concentration. The bound fractions (DFQ) of Na^+ remained roughly unchanged with increasing salt level in the measured samples, as shown in Figure 11. The number of bound Na^+ per surfactant (green open squares and right axis), also plotted in Figure 11, increases from about 40 (3.01% NaCl) to about 80 (5% NaCl). The counterion association and related theories are often studied under relatively low salt-to-surfactant ratios or even in the absence of salt where the degree of counterion binding is limited by the charge of the micelles. In these cases,

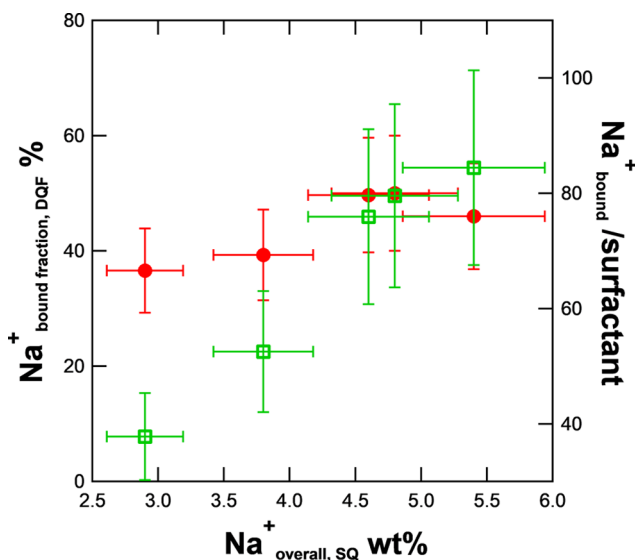


Figure 11. Bound fraction of Na^+ (●) estimated based on DQF measurements and bound Na^+ to surfactant molar ratio (□) vs overall NaCl weight fractions present in the samples measured by SQ NMR. Data points from left to right correspond to surfactant samples with 3.01, 3.56, 4.01, 4.5, and 5% salt. The error bars along the y-axis assume the same accuracy for the DQF measurements as for the SQ ones.

the number of counterions per surfactant is lower than 1.^{50,51} The ion-cloud model, developed from the mathematical result of SANS measurements for samples with high salt-to-surfactant ratios,³³ is based on the assumption that ion binding to the micelle cannot saturate, that is, the charge of the bound counterions can exceed the charge of the surfactants to a great extent. The counterion concentration in the ion-cloud model scales with the increasing salt concentration. The relatively

constant bound fraction of Na^+ with increasing NaCl concentration and the high ratio of bound Na^+ to surfactant as measured by NMR are in agreement with the ion-cloud model developed based on SANS measurements.³³ Further improvement of the ion-cloud model is necessary for better understanding of this special ion behavior and the related thermodynamic impact on micellar systems. The data also suggest the presence of at least two types of sodium ions differing with respect to their mobility, as postulated by the proposed hypothesis. These are preliminary results from a first series of DQF ^{23}Na NMR measurements on a surfactant system with high salt levels. More quantitative measurements will be carried out in future studies.

It is difficult to propose structural or molecular models based on thermodynamic data alone, and one cannot be sure whether all possible impacts have been taken into account. Hence, n_{br}/z was employed to rule out the possible effect of branching and DQF ^{23}Na NMR results to corroborate the presence of excess bound ions. From a structural perspective, ascription of the observed $\frac{d\Delta S_{\text{sc}}}{d\phi_{\text{NaCl}}}$ and $\frac{d\Delta H_{\text{sc}}}{d\phi_{\text{NaCl}}}$ to an increase in hydrophobic hydration at the end caps is the simplest explanation. It would imply that the breakage of WLMs is dominated by the scission of the cylindrical part leading to the formation of two end caps. This occurs in the absence as well as in the presence of branches under the observed experimental conditions.

The SANS model as well as the thermodynamic model employed in this study are surely simplified and of an approximate nature. It is a bit surprising that these simple models yield plausible results. As a continuation of the results presented in ref 13, the applied SANS approach has proven a robust method capable of obtaining verifiable results. For further improvement, a more accurate determination of the scattered intensity $I(q)$ at low q values would be required. The scattered intensity in the low- q region contains information on the WLM contour length. Accordingly, more accurate data at a lower q will provide more accurate values for the number of subunits z and the branch content n_{br} . This would allow testing of more complex theoretical models.

CONCLUSIONS

WLM scission energies ΔF_{sc} have been determined for a mixed surfactant system consisting of SLE1S and CAPB at various temperatures and salt concentrations using SANS and a structural model that allows determination of contour lengths and radii. The enthalpy and entropy of scission were determined by linear fits of ΔF_{sc} as functions of temperature. The energies ΔH_{sc} and $T\Delta S_{\text{sc}}$ decrease with increasing salt concentration. At salt concentrations above 4 wt % of NaCl, ΔS_{sc} adopts negative values. The positive values of ΔS_{sc} can be understood in terms of bound or associated ions, which are released upon scission and formation of hemispherical end caps. The occurrence of negative values of ΔS_{sc} can be explained through a model involving increased hydrophobic hydration of the end caps at high salt concentrations. This hypothesis can explain the decrease in both ΔH_{sc} and ΔS_{sc} . Initial ^{23}Na NMR measurements indicate the presence of immobilized as well as mobile ions, as hypothesized in the previously proposed ion-cloud model. Approaching the WLM system from a structural point of view using SANS in combination with the hybrid wormlike chain scattering function has proven a fruitful method that allows formulation and scrutiny of model-based expectations.

ASSOCIATED CONTENT

Supporting Information

The Supporting Information is available free of charge on the ACS Publications website at DOI: 10.1021/acs.langmuir.8b02930.

Micellar size parameters (Table S1); scattering profiles and fits of studied samples at 15, 25, and 35 °C (Figures S1–S3); scattering profiles of micelles with different geometries (Figure S4) (PDF)

AUTHOR INFORMATION

Corresponding Author

*E-mail: gbeaucage@gmail.com.

ORCID

Karsten Vogtt: 0000-0003-3206-1070

Gregory Beaucage: 0000-0002-6632-0889

Notes

The authors declare no competing financial interest.

ACKNOWLEDGMENTS

This work was funded by P&G. The work relied on the expertise and assistance of Yuri Melnichenko at GP-SANS, ORNL. A portion of this research used resources at the High Flux Isotope Reactor, a DOE Office of Science User Facility operated by the Oak Ridge National Laboratory.

REFERENCES

- (1) Dreiss, C. A. Wormlike micelles: where do we stand? Recent developments, linear rheology and scattering techniques. *Soft Matter* 2007, 3, 956–970.
- (2) Cates, M. E. Dynamics of living polymers and flexible surfactant micelles: scaling laws for dilution. *J. Phys.* 1988, 49, 1593–1600.
- (3) Schramm, L. L. Surfactants: Fundamentals and Applications. In *The Petroleum Industry*; Cambridge University Press: Cambridge, 2000; pp 3–22.
- (4) Nusselder, J. J. H.; Engberts, J. B. Toward a better understanding of the driving force for micelle formation and micellar growth. *J. Colloid Interface Sci.* 1992, 148, 353–361.
- (5) Jiang, H.; Beaucage, G.; Vogtt, K.; Weaver, M. The effect of solvent polarity on the wormlike micelles using dipropylene glycol (DPG) as a cosolvent in an anionic/zwitterionic mixed surfactant system. *J. Colloid Interface Sci.* 2018, 509, 25–31.
- (6) Myers, D. Physical Properties of Surfactants Used in Cosmetics. In *Surfactants in Cosmetics*; CRC Press: Boca Raton, Florida, 1997; pp 29–82.
- (7) Corrin, M. L.; Harkins, W. D. The Effect of Salts on the Critical Concentration for the Formation of Micelles in Colloidal Electrolytes. *J. Am. Chem. Soc.* 1947, 69, 683–688.
- (8) Aswal, V. K.; Goyal, P. S. Counter ions in the growth of ionic micelles in aqueous electrolyte solutions: a small-angle neutron scattering study. *Phys. Rev. E* 2000, 61, 2947–2953.
- (9) Khatory, A.; Lequeux, F.; Kern, F.; Candau, S. J. Linear and nonlinear viscoelasticity of semidilute solutions of wormlike micelles at high salt content. *Langmuir* 1993, 9, 1456–1464.
- (10) Mu, J. H.; Li, G. Z.; Jia, X. L.; Wang, H. X.; Zhang, G. Y. Rheological properties and microstructures of anionic micellar solutions in the presence of different inorganic salts. *J. Phys. Chem. B* 2002, 106, 11685–11693.
- (11) Mukerjee, P. Salt effects on the critical micelle concentrations of nonionic surfactants. *J. Phys. Chem.* 1970, 74, 3824–3826.
- (12) Cates, M. E.; Fielding, S. M. Rheology of giant micelles. *Adv. Phys.* 2006, 55, 799–879.
- (13) Vogtt, K.; Jiang, H.; Beaucage, G.; Weaver, M. Free Energy of Scission for Sodium Laureth-1-Sulfate Wormlike Micelles. *Langmuir* 2017, 33, 1872–1880.

- (14) Candau, S. J.; Hirsch, E.; Zana, R.; Delsanti, M. Rheological properties of semidilute and concentrated aqueous solutions of cetyltrimethylammonium bromide in the presence of potassium bromide. *Langmuir* **1989**, *5*, 1225–1229.
- (15) Candau, S. J.; Merikhi, F.; Waton, G.; Lemarechal, P. Temperature-jump study of elongated micelles of cetyltrimethylammonium bromide. *J. Phys.* **1990**, *51*, 977–989.
- (16) Kern, F.; Zana, R.; Candau, S. J. Rheological properties of semidilute and concentrated aqueous solutions of cetyltrimethylammonium chloride in the presence of sodium salicylate and sodium chloride. *Langmuir* **1991**, *7*, 1344–1351.
- (17) Kern, F.; Lequeux, F.; Zana, R.; Candau, S. J. Dynamical properties of salt-free viscoelastic micellar solutions. *Langmuir* **1994**, *10*, 1714–1723.
- (18) Hassan, P. A.; Valaulikar, B. S.; Manohar, C.; Kern, F.; Bourdieu, L.; Candau, S. J. Vesicle to micelle transition: Rheological investigations. *Langmuir* **1996**, *12*, 4350–4357.
- (19) Soltero, J. F. A.; Puig, J. E.; Manero, O. Rheology of the cetyltrimethylammonium tosylate-water system. 2. Linear viscoelastic regime. *Langmuir* **1996**, *12*, 2654–2662.
- (20) Oda, R.; Narayanan, J.; Hassan, P. A.; Manohar, C.; Salkar, R. A.; Kern, F.; Candau, S. J. Effect of lipophilicity of the counterion on the viscoelasticity of micellar solutions of cationic surfactants. *Langmuir* **1998**, *14*, 4364–4372.
- (21) Raghavan, S. R.; Kaler, E. W. Highly viscoelastic wormlike micellar solutions formed by cationic surfactants with long unsaturated tails. *Langmuir* **2001**, *17*, 300–306.
- (22) Oelschlaeger, C.; Wanton, G.; Candau, S. J. Rheological Behavior of Locally Cylindrical Micelles in Relation to Their Overall Morphology. *Langmuir* **2003**, *19*, 10495–10500.
- (23) Couillet, I.; Hughes, T.; Maitland, G.; Candau, F.; Candau, S. J. Growth and scission energy of wormlike micelles formed by a cationic surfactant with long unsaturated tails. *Langmuir* **2004**, *20*, 9541–9550.
- (24) Siriawatwechakul, W.; LaFleur, T.; Prud'homme, R. K.; Sullivan, P. Effects of organic solvents on the scission energy of rodlike micelles. *Langmuir* **2004**, *20*, 8970–8974.
- (25) Oelschlaeger, C.; Suwita, P.; Willenbacher, N. Effect of counterion binding efficiency on structure and dynamics of wormlike micelles. *Langmuir* **2010**, *26*, 7045–7053.
- (26) Vogtt, K.; Beaucage, G.; Weaver, M.; Jiang, H. Scattering Function for Branched Wormlike Chains. *Langmuir* **2015**, *31*, 8228–8234.
- (27) Abdel-Rahem, R. A.; Reger, M.; Hloucha, M.; Hoffmann, H. Rheology of Aqueous Solutions Containing SLES, CAPB, and Microemulsion: Influence of Cosurfactant and Salt. *J. Dispersion Sci. Technol.* **2014**, *35*, 64–75.
- (28) Nicolas-Morgantini, L. Giant Micelles and Shampoos. In *Giant Micelles: Properties and Applications*; CRC Press: Boca Raton, Florida, 2007; pp 504–509.
- (29) Christov, N. C.; Denkov, N. D.; Kralchevsky, P. A.; Ananthapadmanabhan, K. P.; Lips, A. Synergistic sphere-to-rod micelle transition in mixed solutions of sodium dodecyl sulfate and cocamidopropyl betaine. *Langmuir* **2004**, *20*, 565–571.
- (30) Rosen, M. J.; Zhen, H. Z. Synergism in binary mixtures of surfactants. 7. Synergism in foaming and its relation to other types of synergism. *J. Am. Oil Chem. Soc.* **1988**, *65*, 663–668.
- (31) Cates, M. E.; Candau, S. J. Statics and dynamics of worm-like surfactant micelles. *J. Phys.: Condens. Matter* **1990**, *2*, 6869–6892.
- (32) Kodama, M.; Miura, M. The Second CMC of the Aqueous Solution of Sodium Dodecyl Sulfate. II. Viscosity and Density. *Bull. Chem. Soc. Jpn.* **1972**, *45*, 2265–2269.
- (33) Vogtt, K.; Beaucage, G.; Weaver, M.; Jiang, H. Thermodynamic stability of worm-like solutions. *Soft Matter* **2017**, *13*, 6068–6078.
- (34) Guéron, M.; Weisbuch, G. Polyelectrolyte theory: I. Counterion accumulation, site-binding, and their insensitivity to polyelectrolyte shape in solutions containing finite salt concentrations. *Biopolymers* **1980**, *19*, 353–382.
- (35) Odijk, T. Impact of nonuniform counter ion condensation on the growth of linear charged micelles. *Phys. A* **1991**, *176*, 201–205.
- (36) Odijk, T. Electrostatic interactions in a solution of linear micelles. *J. Chem. Phys.* **1990**, *93*, 5172–5176.
- (37) Tanford, C. The Hydrophobic Effect. In *Formation of Micelles and Biological Membranes*; John Wiley & Sons: New York, 1973; pp 16–23.
- (38) Blokzijl, W.; Engberts, J. B. F. N. Hydrophobic effects. Opinion and facts. *Angew. Chem., Int. Ed.* **1993**, *32*, 1545–1579.
- (39) Southall, N. T.; Dill, K. A.; Haymet, A. D. J. A view of the hydrophobic effect. *J. Phys. Chem. B* **2002**, *106*, 521–533.
- (40) Athawale, M. V.; Sarupria, S.; Garde, S. Enthalpy-entropy contributions to salt and osmolyte effects on molecular-scale hydrophobic hydration and interactions. *J. Phys. Chem. B* **2008**, *112*, 5661–5670.
- (41) Beaucage, G. Approximations Leading to a Unified Exponential/Power-Law Approach to Small-Angle Scattering. *J. Appl. Crystallogr.* **1995**, *28*, 717–728.
- (42) Beaucage, G.; Schaefer, D. Structural studies of complex systems using small-angle scattering: a unified Guinier/power-law approach. *J. Non-Cryst. Solids* **1994**, *172–174*, 797–805.
- (43) Ramachandran, R.; Beaucage, G.; Kulkarni, A. S.; McFaddin, D.; Merrick-Mack, J.; Galiatsatos, V. Branch content of metallocene polyethylene. *Macromolecules* **2009**, *42*, 4746–4750.
- (44) Gobet, M.; Mouaddab, M.; Cayot, N.; Bonny, J. M.; Guichard, E.; Le Quéré, J. L.; Moreau, C.; Foucat, L. The effect of salt content on the structure of iota-carrageenan systems: ²³Na DQF NMR and rheological studies. *Magn. Reson. Chem.* **2009**, *47*, 307–312.
- (45) Mouaddab, M.; Foucat, L.; Donnat, J. P.; Renou, J. P.; Bonny, J. M. Absolute quantification of Na⁺ bound fraction by double-quantum filtered ²³Na NMR spectroscopy. *J. Magn. Reson.* **2007**, *189*, 151–155.
- (46) Allis, J. L.; Seymour, A. M. L.; Radda, G. K. Absolute quantification of intracellular Na⁺ using triple-quantum-filtered sodium-23 NMR. *J. Magn. Reson.* **1991**, *93*, 71–76.
- (47) Boisard, L.; Andriot, I.; Arnould, C.; Achilleos, C.; Salles, C.; Guichard, E. Structure and composition of model cheeses influence sodium NMR mobility, kinetics of sodium release and sodium partition coefficients. *Food Chem.* **2013**, *136*, 1070–1077.
- (48) Okada, K. S.; Lee, Y. Characterization of sodium mobility and binding by ²³Na NMR spectroscopy in a model lipoprotein emulsion gel for sodium reduction. *J. Food Sci.* **2017**, *82*, 1563–1568.
- (49) Purcell, I. P.; Thomas, R. K.; Penfold, J.; Howe, A. M. Adsorption of SDS and PVP at the air/water interface. *Colloids Surf., A* **1995**, *94*, 125–130.
- (50) Manning, G. S. Counterion binding in polyelectrolyte theory. *Acc. Chem. Res.* **1979**, *12*, 443–449.
- (51) Yamabe, T.; Moroi, Y. Micelle formation of anionic surfactant with divalent counterion of separate electric charge. *J. Colloid Interface Sci.* **1999**, *215*, 58–63.